EUROPEAN FUSION DEVELOPMENT AGREEMENT

EFDA–JET–CP(07)03/34

E. de la Luna, L. Barrera, L. Figini, A. Alfier, Y. Andrew, M. Beurskens, D. Farina, E. Giovanozzi, M. Kempenaars, A. Loarte, P. Lomas, C. Mckeena, R. Pasqualotto, G. Saibene, R. Sartori, E.R. Solano and JET EFDA contributors

Measurements of Inboard-Outboard Asymmetry of Pedestal Temperature Collapse during Type I ELMs in JET

Measurements of Inboard-Outboard Asymmetry of Pedestal Temperature Collapse during Type I ELMs in JET

E. de la Luna[1], L. Barrera[1], L. Figini[2], A. Alfier[3], Y. Andrew[4], M. Beurskens[4], D. Farina[2], E. Giovanozzi[5], M. Kempenaars[4], A. Loarte[6], P. Lomas[4], C. Mckeena[4], R. Pasqualotto[3], G. Saibene[6], R. Sartori[6], E.R. Solano[1] and JET EFDA contributors*

[1]Asociación EURATOM-CIEMAT, Avenida Complutense 22, E-28040 Madrid, Spain
[2]Istituto di Fisica de Plasma, CNR, EURATOM-ENEA-CNR Association, Milano, Italy
[3]Associazione EURATOM-ENEA sulla Fusione, Consorzio RFX Padova, Italy
[4]EURATOM-UKAEA Fusion Association, Culham Science Centre, OX14 3DB, Abingdon, OXON, UK
[5]EURATOM-ENEA Fusion Association, C.R. Frascati, CP65, 00044 Frascati, Italy
[6]EFDA Close Support Unit, Garching, Germany
** See annex of M.L. Watkins et al, "Overview of JET Results ", (Proc. 21st IAEA Fusion Energy Conference, Chengdu, China (2006)).*

Preprint of Paper to be submitted for publication in Proceedings of the 34th EPS Conference on Plasma Physics, (Warsaw, Poland 2nd - 6th July 2007)

1. INTRODUCTION

Despite the considerable theoretical and experimental effort, a complete physical model to describe the particle and energy losses during ELMs is far from being complete. On the experimental front, significant progress has been made in characterizing the dynamics and the spatial structure (poloidal asymmetry, radial distribution) of the ELM crash. A number of diagnostics have shown that the ELMs predominantly affect the pressure on the outboard midplane [1, 2, 3], which is consistent with the interpretation of ELM events as ballooning-type instabilities. Much of the effort of the fusion community on this topic has been devoted to measuring the fast evolution of the plasma parameters during the ELM crash. However, there is an obvious need for more profile measurements covering the edge region on the inboard midplane to complement those at the outboard midplane. The objective of this paper is to report on a new set of recent measurements obtained at JET using high spatial and temporal resolution ECE data from both High-Field Side (HFS) and Low-Field-Side (LFS) midplane.Given the relative novelty of the technique, this paper focuses on the validation of the new HFS data and the identification of the limitations of the measurements and the data analysis. Further analysis is required but some preliminary results are presented here.

2. ELECTRON TEMPERATURE PEDESTAL MEASUREMENTS IN JET

The edge electron temperature (T_e) profile in JET is diagnosed with a variety of instruments, including an edge LIDAR Thomson Scattering system [4], an Electron Cyclotron Emission (ECE) radiometer [5] and a recently installed High Resolution Thomson Scattering (HRTS) system [6]. Both the HRTS and the edge LIDAR systems have a nominal spatial resolution of 1.5cm (at the pedestal region), with a repetition rate of 30Hz and 1Hz respectively. The ECE diagnostic consists of 96 closely spaced channels (~1.5cm for the magnetic field gradient in JET) with a spatial resolution (including spectral resolution of the instruments, relativistic broadening of the cyclotron emission and antenna pattern effects) of the order of 3-6cm (depending on plasma conditions and harmonic number). For the experiments reported here a sampling rate of 5kHz was used. The radiometer is cross-calibrated against the absolutely calibrated Michelson interferometer (2^{nd} harmonic, X-mode) during the ohmic phase of the discharge. Although the absolute calibration uncertainties are estimated to be ±10%, the relative systematic errors (estimated from the channel-to-channel variation of assumed-to-be smooth profiles) are of the order of ±5%. In order to compare the profiles form the different diagnostics, measurements are mapped to the mid-plane using EFIT reconstruction.

2.1. ECE MEASUREMENTS: HFS & LFS SIMULTANEOUS T_e MEASUREMENTS

The radiometer in JET consists of 4 independent heterodyne receivers (frequency range from 69 to 139GHz) that can be set up to measure either 1^{st} harmonic/O-mode or 2nd harmonic/X-mode independently. This arrangement was chosen to accommodate the flexibility of JET to operate in a large range of toroidal fields (up to 4T) and allows, for a sub-set of toroidal fields, a combined O- and X-mode operation, giving access to the plasma edge at both HFS and LFS simultaneously.

Access to the inboard edge region is achieved by using O-mode polarization (not affected by harmonic overlapping). The channels at the plasma HFS are calibrated by comparison with the ECE data measured at the plasma LFS during L-mode (assuming that the T_e is constant on a given flux surface). This calibration method has been validated by comparison with the values obtained by crosscalibration with the Michelson interferometer in dedicated toroidal field ramp pulses.

Figure 1 shows an example of the comparison between the T_e profiles measured across the pedestal region with different diagnostics in JET for an ELMy H-mode plasma (B_0 = 2.7T, I_p = 2MA, P_{NBI} = 9MW, P_{ICRH} = 2MW). In general, very good agreement is obtained between ECE and both Thomson Scattering (TS) systems. For high-density plasmas (maximum density limited by cut-off), the location of the ECE channels at the HFS needs to be corrected by taking into account the refraction experienced by the emitted radiation before arriving to the antenna. The effect of the refraction on the T_e profiles is a non-uniform radial shift (increasing towards the plasma centre) that is calculated using a beam tracing code (for the data shown in figure 1, refraction effects were negligible and no correction has been applied).

One of the first observations from the ECE data is the absence of the "enhanced ECE radiation" feature on the HFS profile (more clearly seen in figures 2 and 4). It is generally observed that the radiation temperature (T_{rad}) measured by ECE on the LFS is higher than T_e (derived from TS measurements) with a local maximum appearing at or close to the last close flux surface (R_{LCFS}). This is a well-known ECE instrumental effect that appears systematically in H-mode plasmas (high temperature gradients) and can be attributed to "shine-through" effects due to insufficient optical thickness at the plasma edge. The ECE evaluation assigns the measured value of radiation temperature to the radial position corresponding to the cold resonance location of the emitting frequency. At the plasma edge, the size of the emitting region increases due to the low optical thickness, leading to a shift of the effective measurement position towards the region of higher magnetic field. For the usual case of decreasing temperature towards the edge, this leads to an overestimation of the temperature at the plasma LFS, but not at the HFS. It is also a general observation that the ECE profiles on the LFS are shifted approximately 5cm with respect to the TS profiles. This shift can be corrected by including an error of <1% in the calibration of the *BT* measurements, which is well within the uncertainty of its calibration. A radial shift of 5cm in the ECE data does not only improve the agreement between ECE and TS data but it also brings into alignment the profiles at the plasma HFS and LFS as it can be seen in Fig.1(b). We find that this offset is systematic, and as a result all ECE profiles shown in this paper have been shifted using a correction factor to the total magnetic field. The examples of the T_e profiles shown in this paper illustrate some of the features of the ECE measurements at the HFS. The first thing to notice is that the larger number of points in the HFS profile (smaller channel separation due to higher magnetic field gradient) does not increase the spatial resolution because at each point the emission is limited by the instrumental radial resolution. The spatial resolution of the second harmonic X-mode (~3cm) is better than that of the first harmonic O-mode (~ 6cm) due to its larger optical depth. As a consequence, slightly higher pedestal heights

and gradients (mapped onto the outboard midplane) are calculated from the LFS data, which is the result of the convolution of the real profile with the instrumental resolution of the diagnostic. Temperature collapse during the ELM crash. HFS and LFS comparison A pair of Type I ELMy H-mode plasma discharges with different normalized ELM size: $\Delta T_e/T_{e,ped}$ ~ 0.23 (Pulse No: 69937) and $\Delta T_e/T_{e,ped}$ ~ 0.5 (Pulse No: 69933), where $T_{e,ped}$ is the temperature measured at the top of the pedestal, have been chosen to illustrate the diversity of behaviours observed within the available database. Figures 2 and 4 show the electron temperature profiles, as measured by ECE, shortly before and after one individual ELM event for the two shots mentioned above. Figures 3 and 5 show the temporal evolution of the D_α intensity at the outer divertor and ECE channels for two radial locations (r/a~pedestal top and r/a~0.7) at both HFS and LFS for the same shots. In the analysis presented here it is assumed that the equilibrium and the total magnetic field, that determines the location of the ECE channels, do not change significantly during the ELM crash.

In general, good agreement is observed between the HFS and LFS temperatures before the ELM. However, in the case of the bigger perturbation (see Fig.5), the T_e drop caused by the ELM crash for the inner channels is seen to be smaller in the HFS, leading to a not symmetric collapse of the temperature profile (see Fig.4). Although the systematic errors on ECE data are of the order of ±5%, the parameter that determines the minimum ΔT_e that can be measured is the level of random noise present in the ECE signals, which typically is lower than 50eV. This noise level is small enough to allow a clear determination of the T_e drop due to the ELM crash (see Fig.5(b)). It is found that, for the higher $\Delta T_e/T_{e,ped}$ case, the radial extent of the ELM perturbation (determined by using the temperature profile before and after the ELM) at the outer mid-plane is 40% of the plasma minor radius, while it is only 30% in the inner midplane.

The fast crash of the temperature profile on MHD time scales (~100μs) and the recovery of its pre-ELM value on a time scale of tens of ms are illustrated in figures 3 and 5. For the lower $\Delta T_e/T_{e,ped}$ case, the recovery time of the profile to its pre-ELM value is similar for both the HFS and the LFS. In contrast, for the higher $\Delta T_e/T_{e,ped}$ case, the pedestal temperature on the HFS is seen to recover faster than on the LFS (see Fig.5(c)). One possibility suggested by this experimental observation is that the mapping after the ELM crash may be affected by the plasma movement induced by the loss of beta poloidal due to the ELM. Research is ongoing to investigate this and other sources of uncertainties in the mapping process.

DISCUSSION & CONCLUSIONS

In JET, new detailed measurements of the electron temperature perturbation at both HFS and LFS caused by the ELM crash have been carried out by using high spatial and temporal resolution ECE data. In general, good agreement has been found between the T_e pedestal profiles (before the ELM crash) determined by ECE (both at the HFS and LFS) and the edge LIDAR and HRTS systems. At high densities, refraction effects need to be properly included in the data analysis. The most striking feature noted in comparing the temperature profile evolution before and after the ELM crash is

that, for certain plasma conditions, the ELM affected region is similar for both the LFS and HFS profiles mapped onto the mid-plane. This leads to an asymmetric profile after the ELM crash when mapped onto normalized flux coordinates. Similar results, obtained from the analyses of the collapse of the density profile during the ELM, were obtained previously on ASDEX-U [3]. Within the database analyzed so far, high collisionality (high q_{95}) and high $\Delta T_e/T_{e,ped}$ seems to be the necessary conditions for the appearance of such asymmetry. At present is not entirely clear what the mechanisms are that allows the asymmetry to develop. The extension of the analysis to a larger database and a better understanding of the errors of the mapping process are required in order to determine the plasma conditions under which the inboard/outboard asymmetry in the temperature profiles caused by the ELM event is observed. Detailed analysis of these observations is in progress and it will be addressed in future publications.

REFERENCES

[1]. T.W. Petrie et al., Nuclear Fusion **43** (2003) 910-913

[2]. N. Oyama et al., Nuclear Fusion **44** (2004) 582-592

[3]. I. Nunes et al., Nuclear Fusion **44** (2004) 883-891

[4]. C. Gowers et al., J. Plasma Fusion Res. **76** (2000) 874

[5]. E. de la Luna et al., Rev. Ssi. Instrum. **75** (2004) 3831

[6]. R. Pasqualotto et al., Rev. Sci. Instrum. **75** (2004) 3891

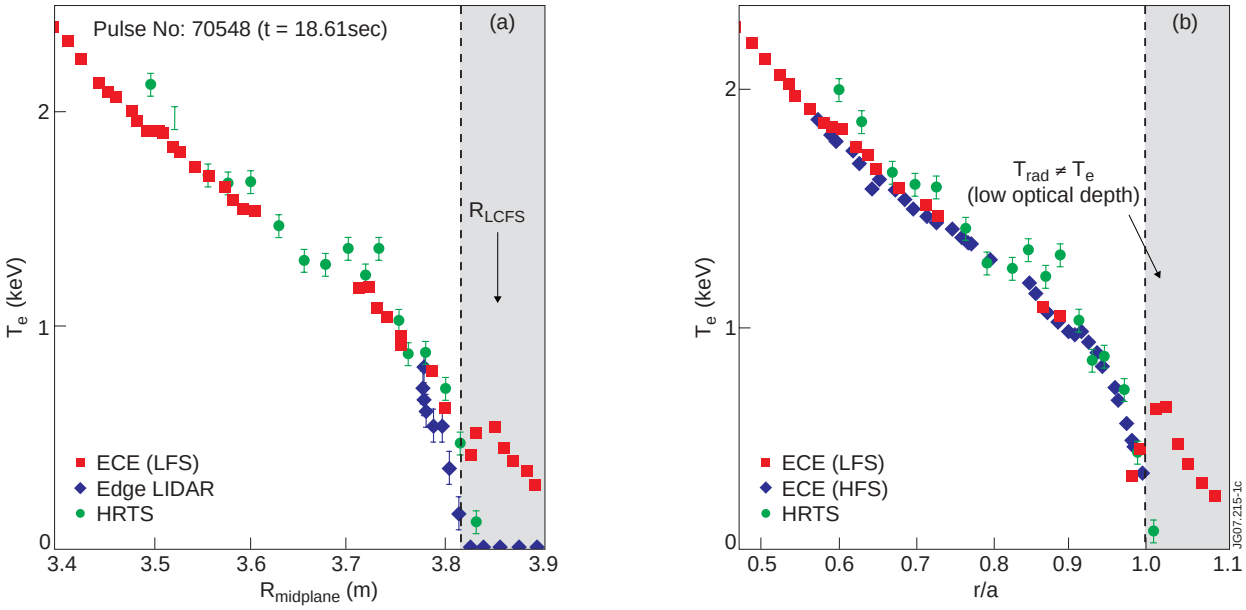

Figure 1: Comparison of the edge T_e profile measured with different diagnostics in JET: a) mapped onto the outboard midplane, b) mapped onto flux coordinates (both HFS and LFS ECE profiles are shown in the figure). The position of the ECE profiles has been calculated increasing the total magnetic field by 0.7%. The arrow in a) marks the maximum of the enhanced ECE radiation region that appears during H-mode on the LFS ECE data. The results of the tanh fits for the ECE/LFS data are shown in the figure (the data with low optical thickness, located within the shaded area in the figures, is not included in the fit).

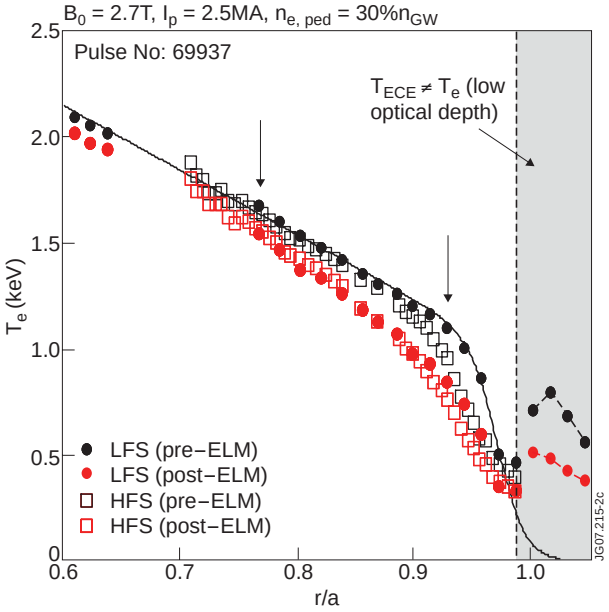

Figure 2: T_e profiles measured by ECE for both HFS (open symbols) and LFS (closed symbols) shortly before (blue) and after (red) one of the individual ELM events shown in Figure 3.

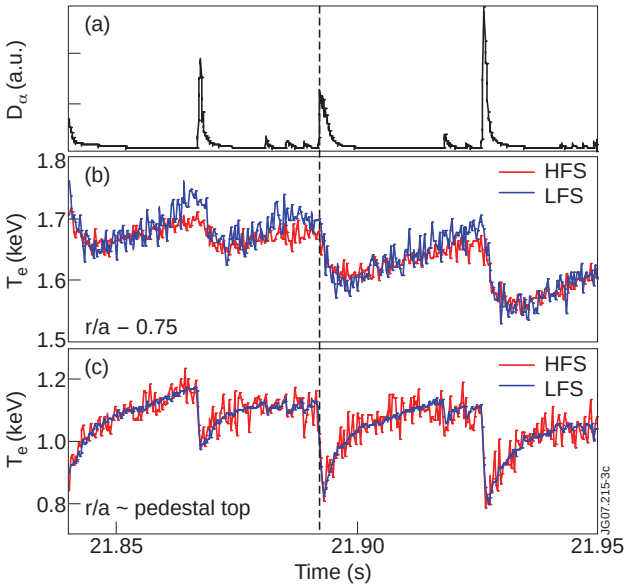

Figure 3: Time evolution of (a) D_α intensity at the outer divertor, T_e, as measured by ECE, at: (b) r/a~0.75 and (c) r/a~$(r/a)_{ped}$ on both HFS (red) and LFS (blue) for Pulse No: 69937 ($\Delta T_e/T_{e,ped}$ ~ 0.23).

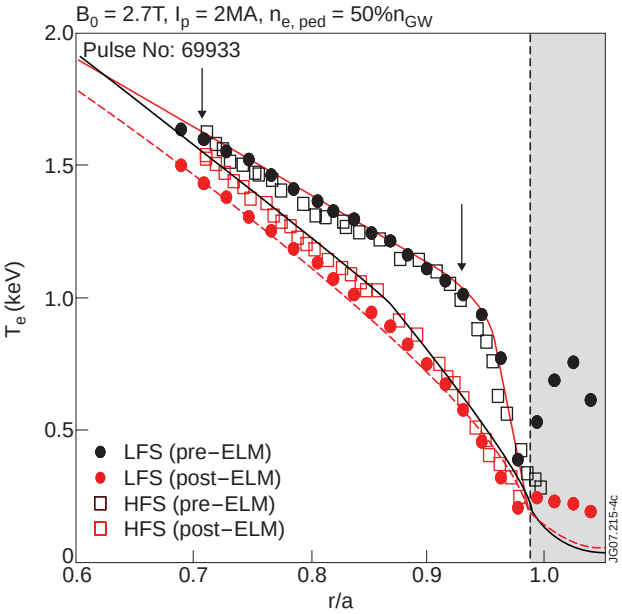

Figure 4: Equivalent to figure 2 but for a plasma discharge with $\Delta T_e/T_{e,ped}$ ~ 0.5.

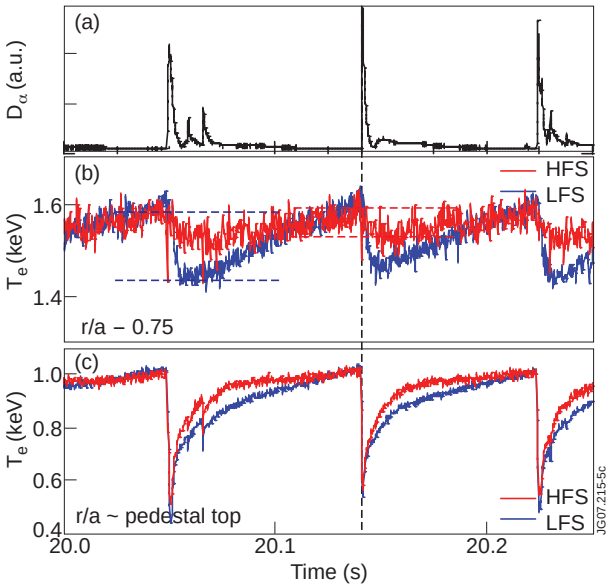

Figure 5: Equivalent to figure 3 but for Pulse No: 69933 ($\Delta T_e/T_{e,ped}$ ~ 0.5).